PVP – Vol. 122

Flow-Induced Vibrations – 1987

edited by
M. K. AU-YANG
S. S. CHEN

PVP - Vol. 122

Flow-Induced Vibrations — 1987

presented at

THE 1987 PRESSURE VESSELS AND PIPING CONFERENCE
SAN DIEGO, CALIFORNIA
JUNE 28 — JULY 2, 1987

sponsored by

THE OPERATIONS, APPLICATIONS, AND
COMPONENTS COMMITTEE,
THE PRESSURE VESSELS AND PIPING DIVISION, ASME

edited by

M. K. AU-YANG
BABCOCK & WILCOX,
NUCLEAR POWER DIVISION
LYNCHBURG, VIRGINIA

S. S. CHEN
ARGONNE NATIONAL LABORATORY
ARGONNE, ILLINOIS

THE AMERICAN SOCIETY OF MECHANICAL ENGINEERS
United Engineering Center 345 East 47th Street New York, N.Y. 10017

Library of Congress Catalog Card Number 86-71376

FOREWORD

This volume contains papers presented at the annual symposium in flow-induced vibration sponsored by the Operations, Applications and Components Committee of the Pressure Vessel and Piping Division of ASME. Altogether, 20 papers from four countries cover a wide range of flow-induced vibration problems in the power generation, process and marine industries. As before, almost half of these 20 papers deals with the dynamics of tube arrays in heat exchangers —probably the most complex of all the flow-induced vibration problems. The editors are particularly pleased to see that, for the first time, there were substantial participation from the People's Republic of China.

The papers can be crudely divided into four categories. Understandably, no clear boundary can be drawn for every paper and some overlapping is unavoidable.

Cross-Flow Induced Vibration of Tube Arrays. Seven papers address this subject. Contents range from fundamental studies to applications of the technology to solving operational problems in the field.

Turbulence-Induced Vibration. Four papers cover this subject, with contents ranging from numerical simulation of the forcing function in tube arrays to response prediction of tubes and shells.

Axial and Annular Flow-Induced Vibration. Five papers present axial flow problems addressing vibration of pipes conveying fluid, large shells exposed to turbulent boundary layers and leakage flow-induced instability of slip joints.

Fluid-Structure and Support-Structure Interaction Effects. Four papers address this subject, which not only includes the much discussed hydrodynamic mass and damping effects but also the all important and often neglected effects of support-structure interaction.

The papers contained in this volume not only represent the latest advances in the state-of-the-art, but also aim at practical applications to design and trouble shooting in the field. The editors wish to express their gratitude for the contributing authors and the reviewers for their time and effort and hope that the symposium on this subject continues to be an annual event in the future. They also wish to thank the Technical Program Chairman A. Marr and the Session Coordinator Dr. J. C. Simonis for their help in organizing this Symposium.

M. K. Au-Yang
S. S. Chen

CONTENTS

DEVELOPMENT OF STABILIZERS FOR STEAM GENERATOR TUBE REPAIR

M. K. Au-Yang
Babock and Wilcox
Nuclear Power Division
Lynchburg, Virginia

ABSTRACT

Fluidelastic stability, turbulence-induced and vortex-induced vibration analysis of different types of stabilizers for repairing steam generator tubes are presented. The performances of the different designs are compared with that of a common basis--the virgin tube. It was found that in addition to permitting the stabilized tubes to remain in operation, the sleeve has the additional merit of being the best performer of all the designs. In addition, it is adaptable to remote installation.

NOMENCLATURE

C_L	Random lift coefficient
D	Outer diameter of tube
f_α	Modal frequency
FSM	Fluidelastic Stability Margin
$G_p^{(i)}$	Power spectral density of turbulence forcing function for i-th span
$J_{\alpha\alpha}^{(i)}$	Joint acceptance for the i-th span for the α-th mode
ℓ	Length of tube
ℓ_i	Length of the i-th span
m	Total linear mass density of tube
m_o	Mean total linear mass density of tube
m,n	Nodal indices
M_α	Generalized mass
U_c	Critical velocity for fluidelastic instability
U_{eg}	Equivalent cross flow gap velocity
α	Modal index
β	Connors' constant
γ	Coherence function
ϕ	Mode shape function
ρ	Fluid density
ρ_o	Mean fluid density
ζ	Damping ratio

INTRODUCTION

During the normal operations of nuclear steam generators, the situation may occur when one or more tubes is degraded by wear, fretting or forms of chemical attack. Once a flaw is initiated, usually at the secondary face of the tubesheets or near the tube support plates, flow-induced vibration may accelerate the degradation. To prevent any possible leakage of the primary fluid, the degraded tubes are usually taken out of service (by plugging) when the flaw size, as determined from eddy current examination, reaches certain predetermined levels. Alternatively, these degraded tubes may be "repaired" by inserting

"sleeves" inside them, thus allowing the degraded tubes to remain operational. Even after the degraded tubes are plugged and taken out of service, the possibility exists that the flaw continues to propagate, resulting in a completely severed tube. To prevent the possibility of a weakened or completely severed tube being excessively excited by the shell-side fluid flow and thus damaging its neighbors, the plugged tubes which are located in regions of high cross-flow are reinforced by "stabilizers." The objective of the stabilizer is to restore the flow-induced vibration (FIV) performance of the degraded and plugged tubes to be equal to or better than that of the original (virgin) tube. Similarly, the sleeve, being a special form of stabilizer, must also be able to restore the FIV performance of a degraded tube to that of the virgin tube.

Thus, the primary objective of stabilizers is to restore the structural integrity of degraded or completely severed steam generator tubes. To achieve this, the stabilizer obviously should be stiff, as well as an effective damper. A continuous solid rod inserted snugly inside a steam generator tube is, in theory, an ideal stabilizer-except for practical installation problems. The stabilizers must be inserted into the tubes from the primary head(s) of the steam generator. Because of the limited clearance between the tubesheet (Fig. 1) and the primary head, a stiff solid rod stabilizer must be made sectional so that it can be inserted and then connected, section by section, into the steam generator tube. The time required to install a stabilizer is directly related to radiation exposure. For this reason, the flexible and the hybrid stabilizers were developed to enable rapid installation in areas of lower cross flows, where sufficient design margins exist.

In the following sections, different stabilizer designs will be discussed and their performances under cross flow-induced vibration will be calculated and compared with that of the virgin tube.

STABILIZER DESIGNS AND SEVER CONDITIONS

As mentioned in the introduction, the basic criteria for a stabilizer are: (1) to restore the structural integrity of a degraded or severed tube and (2) ease of installation. These two requirements unfortunately contradict each other. For this reason, different designs were developed to suit specific applications, as discussed below.

1. The Segmented Solid Rod Stabilizer (Fig. 2a)

This stabilizer is a solid rod constructed in segments to be threaded and crimped together inside the steam generator's primary header. As mentioned earlier, this segmented construction is necessitated by the limited clearance between the primary head and the tubesheet, which also limits the maximum length of each segment. Depending on where the tube defect is located, the length of the stabilizer can be adjusted by connecting different numbers of segments together.

The advantage of the segmented solid rod stabilizer is that it is rigid. However, it does require lengthy installation time in a high radiation environment.

2. The Cable Stabilizer

This stabilizer is basically a flexible cable. The advantage of this design is obvious. Because of its great flexibility, it can be easily bent to clear the header restriction and be inserted into the tubes, making installation time minimal. It was thought that the cable stabilizer might be adequate to repair tubes with defects at the inner surface of the tubesheet. Unfortunately, as the calculations in the following sections show, the cable stabilizer is not sufficient to restore the structural integrity of a degraded tube with respect to flow-induced vibration. Therefore, its development was discontinued.

3. The Laminated Strip Stabilizer (Fig. 2b)

This stabilizer is constructed of three laminated strips stacked (but not attached) together. Because of its laminated construction, the stabilizer is flexible in one direction but fairly stiff in the other. Therefore, this design combines the advantages of the cable and the solid rod stabilizers. On the other hand, the margin against fluidelastic instability is not as large as that of the solid rod stabilizer. The laminated strip stabilizer can be manufactured to arbitrary length and is adequate in regions of lower cross flows.

4. The Hybrid Stabilizer

This stabilizer is a combination of a segmented solid rod stabilizer and a laminated strip stabilizer, with the solid segment extending just beyond the inner face of the tubesheet, where most of the tube defects occur. The flexible portion of the stabilizer usually extends two or more spans. Thus, the hybrid stabilizer offers stiffer structural support to the defective tube than the laminated strip stabilizer but faster installation than the segmented solid rod stabilizer. Its margin against fluidelastic instability is between that of the flexible stabilizer and the solid rod stabilizer.

5. The Sleeve (Fig. 2c)

This stabilizer is a tube with an outer diameter slightly less than the inner diameter of the steam generator tube so that it can be inserted into the latter. By hydraulically or mechanically expanding the sleeve at both ends, the degraded steam generator tube can be "repaired." The sleeve has one great advantage over the other stabilizers - it does not require the degraded tube be plugged so the repaired tube can stay in operation. Furthermore, because the sleeve is semi-flexible, it can be pre-curved to clear the limited space between the tubesheet and the primary head, and then straightened as it is inserted into the tube. A special tool had been developed to perform this remotely, so that the problem of radiation exposure is completely eliminated. (Fig. 3)

FLOW-INDUCED VIBRATION ANALYSIS OF STABILIZERS

As mentioned in the introduction, the primary objective of a stabilizer is to restore the structural integrity, with respect to flow-induced

vibration, of a degraded steam generator tube. While there are many flow-induced vibration mechanisms, some well identified and some still unknown, the best known three are: (1) Fluidelastic instability; (2) Vortex-induced vibration and (3) Turbulence-induced vibration. In this section, the performances of the different stabilizer designs are judged by these three flow-induced vibration phenomena. To check the analytical models used in the calculations and to provide the models with the necessary inputs, simple in-air tests were conducted to measure the stiffnesses, natural frequencies and damping ratios of the stabilizers. Data based on in-air and operational measurements of virgin steam generator tubes showed that [3,4] the in-water (or in-steam) damping ratios were at least as large, so the use of in-air damping ratios in the calculations should be conservative.

To be specific, in the following sections, the qualification of stabilizers designed for applications to the B&W 177FA Once-Through Steam Generators (OTSG, Fig. 1) with the following two tube defects will be discussed.

(1) A tube severed just below the inner surface of the upper tubesheet. This case will be called "tubesheet sever" or TS sever from now on.

(2) A tube severed just above the top (15th) tube support plate. This case will be called "15th tube support plate sever" or 15th TSP sever from now on.

The reason for choosing these two faulted conditions for analysis is that in an OTSG, these two locations have experienced degradation. In addition, the top span of the steam generator tube is subject to the highest cross flow. Thus, these two cases will serve as an upper bound for applications of the stabilizer. Other faulted conditions can be analyzed similarly.

The following stabilizers will be included in the following analysis:

(1) A one-span solid rod stabilizer consisting of segments extending just beyond the lower surface of the 15th tube support plate.

(2) A two-span solid rod stabilizer similar to the above except it extends just beyond the bottom of the 14th TSP.

(3) A two-span laminated stabilizer similar to the above.

(4) A hybrid stabilizer consisting of standard solid rod segments at the top followed by a standard laminated stabilizer.

(5) A sleeve stabilizer, which is a tube with outer diameter slightly smaller than the inner diameter of the steam generator tube, so that it can be inserted into the tube and extend beyond the 15th TSP.

(6) A cable stabilizer equal in length and diameter to the two-span, solid rod stabilizer but is completely flexible, i.e., it has a zero moment of inertia.

In addition, the virgin (un-blemished) tube is also analyzed and the results are used as the basis for comparison. The dimensions of the virgin tube are: OD = 0.625 in. (1.5875 cm) with a wall thickness of 0.034 in. (0.86 mm).

The material for all stabilizers is assumed to be the same as that of the virgin tube: Inconel 600, with Young's modulus (at 600°F) equal to 29.2×10^6 psi (2.013×10^5 MPa), a Poisson ratio of 0.3 and density equal to 7.93×10^{-4} lb-s^2/in^4 (8481.5 Kg/cu.m.).

With the exception of the sleeve when used as a repair, each stabilizer is mechanically attached to a plug. The stabilized tubes will be removed from operation by this plug. When the sleeve is used as a stabilizer, it may also be mechanically attached to a plug and the assembly remotely installed.

1. In-Air Test

To provide the analysis with the necessary input damping ratios and stiffnesses and to check the assumed boundary conditions of the analytical model, a simple model consisting of the top three spans of the OTSG tube and the stabilizer was tested in air. Fig. 4 is a sketch of the fixture used to perform the test. It consisted of a heavy beam anchored to the floor by a hinge so that it could be lowered to change stabilizers; the beam was positioned vertically during the test. The upper tubesheet was simulated by a two-foot (60.96 cm) clamp split along its length and was anchored to one end of the beam. When bolted together, the clamp provided sufficient fixity to the tube to simulate a clamped boundary condition at the upper tubesheet. In addition, a 6.3 mil (0.16 mm) shim stock was wrapped around the tube at the bottom of the tubesheet to further clamp the tube.

The support plates were spaced along the beam exactly as in the steam generator. However, instead of using broached holes as in the steam generator, the tubes were silver soldered to 10 mil (0.254 mm) shim stocks that were in turn welded to square frames to simulate the tube support plates. This arrangement eliminated tube-to-support plate impacting, which could cloud the damping measurements so that direct comparisons between stabilizers of different designs would be difficult.

The tube or tube/stabilizer was excited in two different ways. For steady state tests, it was excited by a 50-lb (222.4-N) electromagnetic shaker mounted at the middle of the top span and was attached to the tube with a low mass aluminum grip. For transient tests, the shaker was removed and the tube was excited either by plucking or by impacting with a light hammer.

The responses of the tube or tube/stabilizer combination were measured by a non-contacting displacement probe mounted below the shaker. Flat targets were clamped on the tube to measure its displacements in the in-plane and out-of-plane directions. In all cases, the probe was calibrated before use and it was found necessary to remove the D.C. component of its signal before recording by 2.0 Hz high-pass filters.

The information derived from the simple in-air test were static stiffness, fundamental modal frequencies and damping ratios. The static stiffness was determined by attaching a static load cell to the tube. By pulling the tube with the load cell to discrete displacement steps, a load deflection curve was obtained. The static stiffness was obtained by fitting a straight line through these data points. The modal frequencies were determined by standard spectral analysis using a commercial Fourier analyzer. Two methods were used to determine the damping ratios: the half-power point method using data from the steady state shaker test, and the logarithmic decrement method using the transient (pluck or impact) test data. The results will be given in the following sections on qualification analysis.

2. Fluidelastic Stability Analysis

As its name implies, the primary objective of a stabilizer is to restore stability to the degraded or severed tube, so that it would not undergo whirling due to cross flow (Connors' mechanism) and hit its neighbors. To judge the performances of stabilizers of different designs, we calculate the "fluidelastic stability margin" (FSM)[1], defined as the ratio of Connors' critical velocity to the mode shape weighted effective cross flow gap velocity.

$$FSM = U_c/U_{eg}$$

Where

$$U_c = \beta f_n \sqrt{2\pi\zeta m/\rho}$$

is Connors' critical velocity and,

$$U_{eg}^2 = \left[\frac{1}{\rho_o}\int_o^{\ell} \rho(x)U_g^2(x)\phi_n^2(x)dx\right]\left[\frac{1}{m_o}\int_o^{\ell} m(x)\phi_n^2(x)dx\right]^{-1}$$

is the mode-shape weighted equivalent cross-flow gap velocity. Theoretically, FSM < 1 implies the tubes will be unstable while FSM > 1 implies the tube will be stable. In practice, because of the uncertainties in the input damping ratios, Connors' constants and the like, the above conclusions are not necessarily true. However, for the design of stabilizers, precise knowledge of these inputs are not necessary since the analysis is a comparative one based on an accepted condition (that of the virgin tube). If the stabilized tube has a fluidelastic stability margin equal to or larger than that of the corresponding virgin tube, then its design objective is met -- the repaired tube will be at least as stable as the original tube. Furthermore, the larger the computed FSM, the larger the margin of safety (with respect to fluidelastic instability). Thus, the performances of stabilizers of different designs can be compared by comparing their computed FSMs. The uncertainty in the input Connors' constant cancel out because we are dealing with the same bundle geometry in each case.

The virgin tube was modelled as a continuous beam pin-supported at each of the tube support plates and clamped at the inner surfaces of the upper and lower tubesheet. The justification of the latter boundary condition is the small nominal diametric clearance between the tube and the tubesheet. For large deflections (more than 100 mils, or 2.5 mm peak to peak) experienced during fluidelastic instability, the tube will pick up additional support inside the tubesheet. The boundary condition at the tubesheet thus approaches that of being clamped. The non-structural mass, which is equal to the sum of the mass of the fluid inside the tube and the virtual mass, was included in the model. By interpolation of experimental data from Ref.[2], it was found that the virtual mass in the present case was about three times the mass of fluid the tube displaces.

The sever condition was modelled by putting the shear and moment carrying capability of the tube equal to zero at the sever location. Each stabilizer was modelled again as a beam fixed at the top of and pinned at the bottom of the tube sheet. Below the tubesheet, each stabilizer node was tied rigidly in shear to the corresponding tube node with the multi-point constraint equations in the computer program NASTRAN.

The laminated stabilizer was modelled as an equivalent single beam with moment of inertia equal to the sum of the moments of inertia of the three individual strips. The segmented rod stabilizer was modelled as a continuous solid rod. The change in stiffnesses at the threaded joints was ignored in the analysis, since tests had demonstrated that it is not significant.

Before being applied to the steam generator, the above modelling technique was first checked against the test setup. Table 1 lists the computed and measured natural frequencies and stiffnesses of a tube severed at the tubesheet and stabilized with a one-span solid rod or a two-span laminated stabilizer.

Table 1. Comparison Between Calculated and Measured Natural Frequencies and Stiffness

Stabilizer in Test Setup	Stiffness (lb/in) Calc.	Stiffness (lb/in) Meas.	Frequencies (Hz) Calc.	Frequencies (Hz) Meas.
Two Span Laminated	79.6	81.5	24.6	20.4
One-Span Solid	169.3	115.7	29.4	16.9-28.3

Agreements between calculated and measured results ranged from fair to good. The large test data scatter in the natural frequencies of the solid-rod stabilized tube was believed to have been caused by the intermittent contact between the tube and the stabilizer noted during the test in the form of rattling sounds. As the displacements became larger, more positive contact between the tube and the solid rod stabilizer was established and the measured natural frequencies approached the theoretical value. This rattling was not observed in the laminated stabilizer because of its construction--the individual strips

tended to "fill" the tube, giving it a more positive support even at relatively small deflections.

The assumed damping ratios in the calculation of FSM were derived from tests and are given in Table 2 as multiples of the damping ratio for that of the virgin tube.

3. Results from Fluidelastic Stability Analysis

Table 2 lists the input damping ratios and the natural frequencies of the least stable (and thus the determining) mode, together with the computed fluidelastic stability margins (FSM) for (1) A virgin tube; (2) A tube severed at the tubesheet and supported by one of the stabilizers; and (3) a tube severed at the 15th TSP and supported by one of the stabilizers. In each case, the Connors' constant was the same. The tube considered was one located at the point of highest cross flow. Representative mode shapes of the virgin tube and some of the stabilized tubes are shown in Fig. 5.

4. Turbulence-Induced Vibration Analysis

Unlike fluidelastic instability which can be avoided by design, turbulence-induced vibration always exists wherever there is flow over a flexible structure. Thus, even if the repaired tube is stable, care still has to be taken to assure that the stabilizer does not significantly increase its turbulence-induced vibration amplitude (and hence stress). Two methods were used to evaluate the random vibration amplitudes and stresses of the virgin and the stabilized, severed tube. Both methods gave similar results.

The first is the acceptance integral method generalized to a multi-span tube with non-uniform total linear mass density. It was shown in Ref.[5] that the mean square vibration amplitude at any point on a multiply-supported tube is given by:

$$\bar{y}^2 \approx \sum_{\alpha} \sum_{i} \frac{\ell_i G_p^{(i)}(f_\alpha)\phi_a^2(x)}{64\pi^3 M_\alpha^2 f_\alpha^3 \xi_\alpha} \int_o^{\ell_i} \phi_\alpha^2(x)dx. \quad J_{\alpha\alpha}^{(i)}$$

Where $J_{\alpha\alpha}^{(i)}$ is the joint acceptance for the i-th span. In general, $J_{\alpha\alpha}^{(i)} < 1.0$ so the choice of $J = 1.0$ for all modes (α) and all spans (i) over which there is cross flow will give an upper bound estimate of the vibration amplitude of the tube.

The second is the coherence integral method. It was shown in Ref.[6] that under the assumption that the flow is fully coherent within each span (i.e. $J = 1.0$) and is completely incoherent across different spans (same assumption as in the first method), then the coherence matrix elements are given by,

$\gamma_{mn} = 0$ for nodes m,n not in the same span

$\gamma_{mn} = dx_m dx_n$ for nodes m,n in the same span

where dx_m, dx_n are finite element lengths. Thus, the coherence integral can be calculated separately and its matrix element input into the finite element computer program NASTRAN, which is then used to compute the responses and stresses.

In both methods, the excitation power spectral density due to the cross flow was computed from the random lift coefficient [7],

$$G_p^{(i)}(f) = \left\{\frac{D^2}{2^2} C_L^2(f) \int_o^{\ell_i} \left[\rho(x)U_g^2(x)\right]^2 \phi_\alpha^2(x)dx\right\} \cdot \left\{\int_o^{\ell_i} \phi_\alpha{}^2(x)dx\right\}^{-1}$$

We used the maximum value from Fig. 10 of Ref.[7] for the random lift coefficient:

$$C_L = 0.025.$$

The damping ratios are the same as those used in the stability calculations.

5. Results from Turbulence-Induced Vibration Analysis

Table 3 lists the computed maximum vibration amplitudes and bending stresses in the top span for (1) a virgin tube; (2) a tube severed at the tubesheet and supported by one of the stabilizers and (3) a tube severed at the 15th TSP and supported by one of the stabilizers. As in the stability calculation, the tube considered is the one subjected to the highest cross flow, i.e., one located by the lane and on the 4th row from the periphery.

6. Vortex-Induced Vibration Analysis

As discussed in Ref. [5], vortex shedding in a tube bundle is much less clearly defined than in a single cylinder. Experimental measurements involving tube bundles indicated that even if a resonance peak existed in the dynamic pressure power spectral density, it was much broader and not as well defined as in cross flows over an isolated cylinder. The dynamic pressure PSDs in a tube bundle often bound these pseudo deterministic peaks. However, if lock-in vortex-induced vibration occurs for a particular mode in a particular span, then the forcing function becomes fully correlated with the mode shape in that span. This means that the span acceptance integral $J = 1.0$; or the coherence integral matrix element equals $dx_m dx_n$. This is exactly what we assumed in the turbulence-induced vibration analysis in the previous section. In other words, our turbulence-induced vibration analysis assumes that lock-in, vortex-induced vibration occurred at every of the twenty modes included in the analysis, and over every span where there is cross flow. Since it is extremely unlikely this can happen in practice, the results in the previous section not only are very conservative for turbulence-induced vibration, but they are conservative for vortex-induced vibration as well. Thus, no separate vortex-induced vibration analysis is necessary.

Table 2. Comparison of Fluidelastic Stability Performances of Stabilizers

Stabilizer	Damping Ratio	TS Sever Freq (Hz)	TS Sever FSM	15th SP Sever Freq (Hz)	15th SP Sever FSM
Virgin Tube	zeta	42.2	1.34	(No Sever)	
1-Span solid	3.33 zeta	28.7	1.64	----	----
2-Span solid	3.33 zeta	29.4	1.76	34.6	2.38
2-Span laminated	2.33 zeta	20.2	0.88	26.8	1.30
Hybrid	2.67 zeta	24.6	1.31	28.7	1.80
Sleeve	2.00 zeta	39.0	1.67	32.2	2.22
Cable	5.00 zeta	6.0	0.68	-----	----

Table 3. Comparison of Turbulence-Induced Vibration and Stress Amplitudes**

Stabilizer	TS Sever RMS Displ. (in)	TS Sever RMS Stress* (psi)	15 SP Sever RMS Displ. (in)	15 SP Sever RMS Stress* (psi)
Virgin Tube	.018(no sever)	1800(no sever)		
1-span solid	.010	<1000	---	---
2-span solid	.010	<1000	<.010	<1000
2-span laminated	.045	1800	.027	2600
Hybrid	.019	<1000	.012	1200
Sleeve	.013	<1000 (tube)	.0082	<1000 (tube)
		1900 (sleeve)		<1000 (sleeve)

*This is the maximum tube stress, occurred at the tubesheet
**Maximum displacement is at center of top span

DISCUSSION OF RESULTS

Table 2 compares the fluidelastic stability performances of the different stabilizers. It isimmediately apparent that the sleeve is, by a wide margin, the best performer in this area. After it is stabilized by a sleeve, a tube severed either at the TS or at the 15th TSP, and hence most likely anywhere in between, will be even more stable than the original tube. The sleeve has other advantages - its semi-flexible characteristic enables it to be installed remotely; and its tubular construction enables the repaired tube to remain in service whereas the tube must be plugged and removed from service when other stabilizers are used.

As far as stability is concerned, the two span segmented solid rod stabilizer offers even better performance than the sleeve, but not by much. It is the most obvious design to restore stability to a severed tube. However, its sectional construction requires long installation time and hence large radiation exposure -a major drawback.

The one-span segmented solid rod stabilizer was designed to reduce the installation time (and hence radiation exposure). Table 2 shows that for sever at the tubesheet, it works almost as well as the two-span stabilizer. However, it has not been used when the tube defects are near the 15th TSP.

The laminated stabilizer is designed for rapid installation -- due largely to its flexibility in one of the two directions. However, since in actual application, neither the orientation of the stabilizer nor the direction of the cross flow can be precisely controlled, the stabilizing effect of the laminated stabilizer must be determined by the less stiff direction to be conservative. It has been shown that the larger stiffness in the perpendicular direction generally helps the stability in the weaker direction. The calculation shows that the laminated stabilizer cannot restore the FSM of a tube severed at the tubesheet to that of a virgin tube. However, when the sever is at the 15th TSP, the laminated stabilizer can restore the FSM of the tube to almost that of the virgin tube.

Therefore, the laminated stabilizer can be used as long as the sever is near the 15th TSP. When the sever is at the tubesheet, the laminated stabilizer can be used only if the tube is located in regions of lower cross flow velocity. If we want the stabilized tube to have an FSM equal to or larger than that of a virgin tube at the location of highest cross flow (FSM = 1.34), then the average cross flow velocity over this tube should not exceed 0.88/1.34 = 2/3, the maximum mean cross flow velocity in the bundle. This gives an exclusion zone within which the laminated stabilizer should not be used if the sever is at the tubesheet to maintain the same fluidelastic stability margin as the original tube.

The hybrid stabilizer was designed to take advantage of the excellent stiffening effect of the solid rod stabilizer and yet permits much faster installation. By extending the solid section just beyond the tubesheet, this design greatly improves the stabilizing ability of the laminated stabilizer, especially for tubes severed at the tubesheet. Yet, because most of the stabilizer is flexible, it can be installed much faster than the solid rod stabilizer.

If rapid installation were the only criterion in a stabilizer design, then the most obvious design would be a completely flexible cable, which can be easily bent to conform with the internal shape of the primary head and be inserted through the tubesheet into the damaged tube. Unfortunately as Table 2 shows, the cable stabilizer offers disappointing stability performance even if its damping ratio were five times that of the virgin tube. Therefore, further development of the cable stabilizer was discontinued.

A tube subject to cross flow always experiences wear and fretting and possibly fatigue damage due to turbulence-induced or vortex-induced vibration. For the same geometry and under the same environment, it is generally true that a tube that vibrates more is more prone to be damaged by fretting, wear and fatigue. Therefore, even if the repaired tube is stable, one must make sure that the same tube will not have unacceptably high turbulence or vortex-induced vibratory responses. As Table 3 shows, the sleeve again excels in this area. A tube severed either at the TS or the 15th TSP and stabilized by a sleeve will have smaller turbulence or vortex-induced vibrational motion and stress. Hence, it is less susceptible to fatigue, fretting and wear than the virgin tube. The estimated stress induced in the sleeve itself, is also acceptably small, being approximately the same as that of the virgin tube. Almost as good are the 1-span or 2-span solid rod and the hybrid stabilizers. The laminated-strip stabilizer, on the other hand, cannot restore a severed tube to the original condition with respect to turbulence-induced or vortex-induced vibration. However, the responses are still small and is unlikely to be a problem.

SUMMARY REMARKS AND CONCLUSION

The performances of the various stabilizers are largely determined by their performances with respect to fluidelastic instability. In all cases, turbulence-induced or vortex-induced vibration amplitudes and stresses of the stabilized tubes are small -- often smaller than those in the virgin tube.

Even though the solid rod stabilizer is the most obvious design, and is in fact, the first design used in the field, it suffers from the long time necessary for its installation. The completely flexible cable obviously requires the least installation time. Unfortunately it does not offer sufficient stiffening effect to the severed tubes. The laminated strip stabilizer offers sufficient flexibility for rapid installation and better fluidelastic stability performance than the flexible cable. It is adequate for most applications where the severed tube is not at the locations of highest cross flow. The hybrid stabilizer combines a solid rod stabilizer at the top with a laminated "tail". It offers reasonably fast installation time and adequate stabilizing effect for both sever conditions considered. However, the best design appears to be the sleeve. Not only that a sleeved tube can remain in service whereas all other stabilizers require that the repaired tube be plugged and removed from service, but the sleeved tube actually has more fluidelastic stability margin and less turbulence-induced stress than the original tube. In addition, it can be installed remotely, thus avoiding any radiation exposure.

In the past ten years over 500 sleeves and over 1000 solid rods, laminated strip and hybrid stabilizers had been installed in both once-through and re-circulation type steam generators. So far, no operational problems have been encountered in any of the stabilized tubes.

ACKNOWLEDGEMENT

The author wishes to express his gratitude to Messrs. B. Brenneman and K.P. Maynard for their contributions to the calculations in this paper. This program was developed under the leadership of Mr. J.E. Gutzwiller, Manager of Steam Generator Engineering at Babcock & Wilcox's Nuclear Power Division.

REFERENCE

1. Au-Yang, M.K.; "Flow-Induced Vibration: Guidelines for Design, Diagnosis, and Trouble Shooting of Common Power Plant Components," ASME Transaction, J. Pressure Vessel Tech., v.107, 1985, pp. 326-334.

2. Chen, S.S., et al., "Experiments in Fluidelastic Vibrations of Tube Arrays," Argonne National Laboratory Report No. ANL-CT-&&-16, Apr. 1977.

3. MacDonald, M.P.; Roman, G.W.; "TVA IEOTSG In-Air Test," B&W Alliance Research Center Report No. RDD:83:2043-07-01, March 1984.

4. Johnsen, J.R.; "Flow-Induced Vibration Analysis of the Three-Mile Island Unit-2 Once-Through Steam Generator Tubes," EPRI Report No. NP-1876, June 1981.

5. Au-Yang, M.K.; "Turbulent Buffeting of a Multispan Tube Bundle," ASME Transaction, J. Vibration, Stress and Reliability in Design, v.108, April 1986, pp.150-154.

6. Brenneman, B.; "Random Vibration due to Small Scale Turbulence with the Coherence Integral Method," paper submitted for publication.

7. Paidoussis, M.P.; " A Review of Flow-Induced Vibrations in Reactors and Reactor Components," Nuclear Engr. and Design, v.74, 1983, pp.31-60.

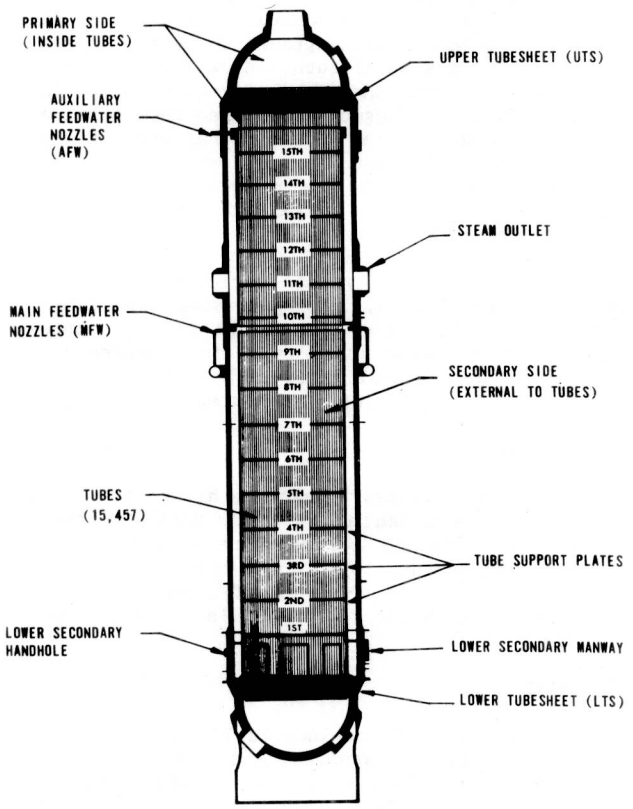

Figure 1. Schematic Drawing of an Once-Through Steam Generator (OTSG)

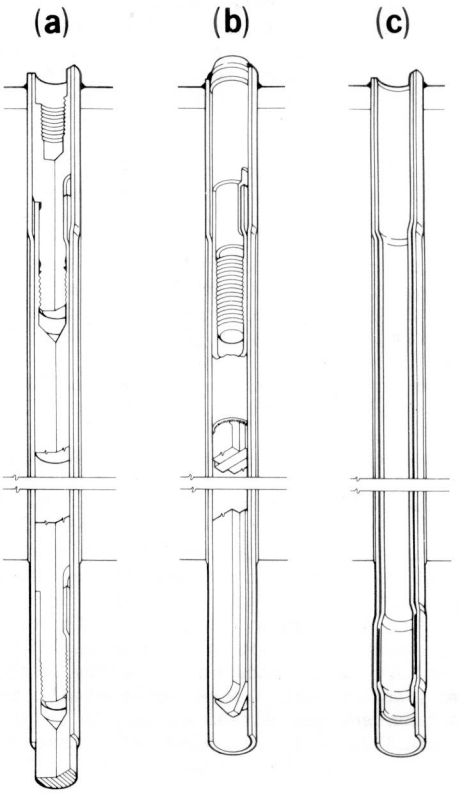

Figure 2. Three Different Stabilizer Designs: (a) The Segmented Solid Rod Shown With the The Plug; (b) The Laminated Strip Shown With the Plug and (c) The Sleeve.

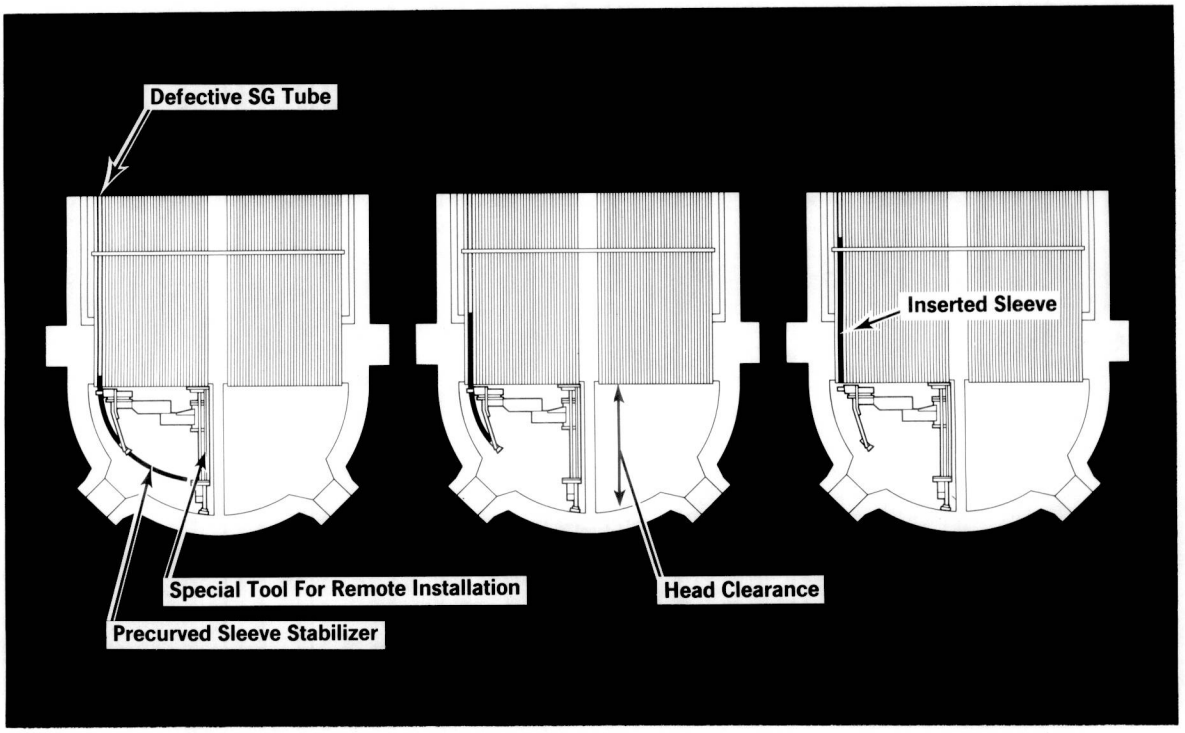

Figure 3. Remote Installation of a Sleeve Stabilizer into a Steam Generator

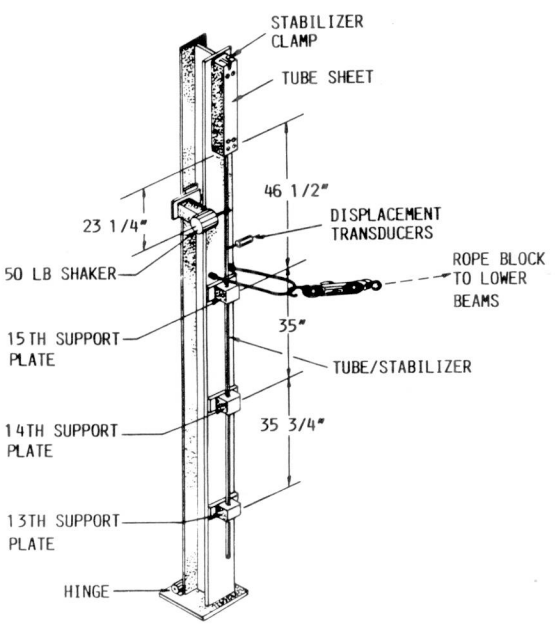

Figure 4. In-Air Test Set-Up

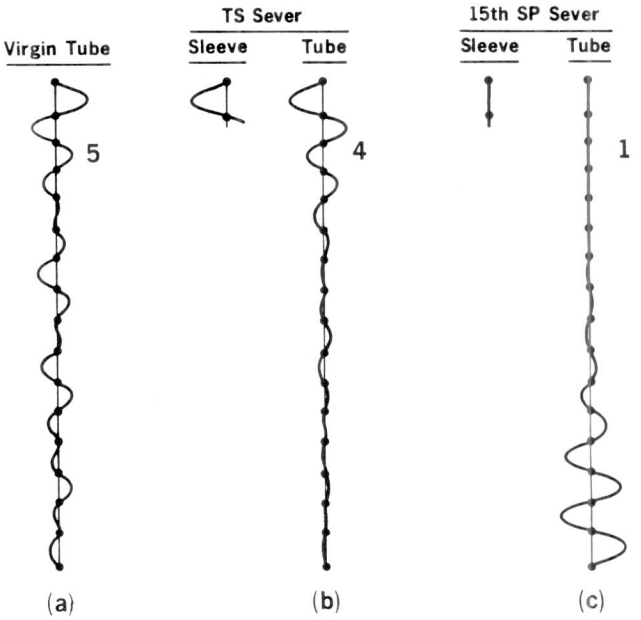

Figure 5. The Least Stable Modes: (a) 5th Mode of the Virgin Tube; (b) 4th Mode of TS Severed Tube with Sleeve and (c) 1st Mode of 15th TSP Severed Tube with Sleeve.

THEORETICAL AND EXPERIMENTAL STUDIES ON FLUIDELASTIC VIBRATION OF TUBE TANK IN A LARGE EVAPORATOR

Xiao-ming Ma, Master of Engineering, **Song-wen Qian**, Professor, **Han-Zhao Cen**, Associate Professor and **Wen-ming Zen**, Lecturer
Department of Chemical Engineering Machinery
South China Institute of Technology
Guang-Zhou, Guangdong, China

ABSTRACT

According to fluid inertial mechanism, tube equation of motion and its solution are deduced. A design criterion is then presented and its relevant equation is obtained. Meanwhile, two new dimensionless parameters are given: the " equivalent Strouhal Number "β, and the " universal flow-induced vibration parameter "ξ, both reflecting nearly all the factors concerned with tube vibration. Within the range of $m\delta/(\rho d^2)$ from 30 to 1000, theoretical results show good agreement with formulas proposed by Pettigrew et al. Full-scale test of a large evaporator shows that some measured results are different from those obtained from idealized model.

NOMENCLATURE

d_i, d_o =tube inside and outside diameters: m;
E =Young's modulus of tube material: P_a;
f =frequency of tube vibration: Hz;
g =gravitational acceleration constant;
K =fluidelastic instability constant, dimensionless;
l_t=tube total length: m;
r =frequency constant: dimensionless;
s =distance along streamtube to the inlet :m;
t =time: sec. ;
U_p, U_o =pitch velocity and steady flow velocity at the inlet : m/s;
U, u =steady and perturbation magnitudes of flow velocity: m/s;
θ =phase angle(or lag): deg. ;
δ =logarithmic decrement of damping: dimensionless;
ρ =fluid density: kg/m^3;
ω =angular frequency of tube vibration: 1/sec. ;
i =subscript variable: integer.

INTRODUCTION

Recently, with rapid developments in power, nuclear and other industries, good overall performances of heat exchangers are required. The appearance of large and high performance heat exchangers has brought about more and more problems concerned with flow induced tube vibration (1-5,7).

After 30 years' of study(3), three main mechanisms have been proposed, i.e, vortex shedding, turbulent buffeting and fluidelastic instability. They are used as design criterion(4). Owing to the complexity of the problem itself, the traditional way for the researchers is to conduct an idealized test on a scaled model and obtain an empirical or semi-empirical formula.

The associated parameters and factors give the designers the problem of how to have a good choice. For this reason, a design criterion is presented after theoretical analysis and full-scale experiment on a large evaporator which once had severe tube damage due to flow induced vibration

THEORY

1. Equation of Motion

Under service conditions, cross-flow induced vibration of heat exchanger tubes is very complicated. Tubes are subjected to lift force, drag force, direct striking force and fluidelastic stiffness force. Tube vibration is affected by multiple factors such as the stiffness of the tube assembly, structural damping, material damping, fluid dampings inside and outside the tubes, coupling between the tubes and the fluid as well as their neighbouring tubes,etc. For the convenience of analysis, the following assumptions are made(1,5):

(a) The tubes are assumed to be straight Euler-Bernoulli beams with the same cross-section areas, and undergo simple harmonic motion in the lift direction only.

(b) The flow distribution at the inlet is assumed uniform, and there exist two streamtubes symmetrically around a single flexible tube as shown in Fig.(2), the flow is one-dimensional in the streamtubes. Detailed explanations of above two assumptions are in references(1,5).

1.1 Analytical Model. Tubes in this evaporator are single-spanned. Their physical and mathematical model is shown in Fig.(3).

1.2 Fluid Excitation Force $F_f(z,t)$. Based on fluid redistribution mechanism, the relationships between tube motions and the change of physical variables of streamtubes are considered as follows:

(1) Streamtube Area A(s,t). From the assumptions above, the tube in Fig.(2) undergoes single harmonic motion $y=y_o\sin t$ in the lift direction only. Streamtubes are formed by fixed boundaries and steady streamlines. Assume streamtube areas to vary with s and t, and both of the two areas have the same form of expressions as tube motion. From the geometries and mathematical deductions, the following area function is obtained:

$$A_i(s,t)=\bar{A}(s)+(-1)^{i+1}a(s)\sin(\omega t+2\omega s/U_o) \quad ...(1)$$

where, $\bar{A}(s)$,$a(s)$ are the steady-state streamtube area and the area perturbation magnitude, respectively. $2\omega s/U_o$ is the phase lag between the tube motion and the resulting flow area change at section s.

(2) Flow Velocity $U_i(s,t)$. The Mach Number of the shell side fluid under service and test conditions is less than 0.4. So that the flow may be considered as incompressible(8). Suppose the streamtube velocity to have the same function form as areas, i.e,

$$U_i(s,t)=\bar{U}_i(s)+u_i(s)\sin(\omega t+\phi_i(s)) \quad ...(2)$$

Consider streamtube 1, and apply the one-dimensional unsteady continuity equation to the incompressible fluid flowing through the streamtube:

$$\frac{\partial A_1(s,t)}{\partial t}+\frac{\partial}{\partial s}\left[A_1(s,t)\cdot U_1(s,t)\right]=0 \quad ...(3)$$

Replacing $A_1(s,t)$, $U_1(s,t)$ in equation (3) by equations (1) and (2), and setting steady state area A_{10} at the inlet to equal to $\bar{A}_1(s)$ for all s, and then neglecting the higher-order components, the following equation is obtained by the integration of equation (3) from the inlet to s

$$U_1(s,t)=U_{10}+\frac{3U_oy_o}{A_{10}}\sin[\omega(s+s_o)/U_o]\sin[\omega t+\omega(s-s_o)/U_o-\tfrac{1}{2}\pi] \quad ...(4)$$

(3) Fluid Excitation Force $F_f(z,t)$. Following the method mentioned above, by assuming streamtube pressure function and the use of momentum equation to the streamtube, the amplitude and phase lag of pressure variation may be deduced. The fluid force acting on unit length of tubes at the inlet is the integration of pressure distribution along the two streamlines in Fig.(2). This yields:

$$F_f(t)=F_o\sin(\omega t+\theta_o) \quad ...(5)$$